







# Discovery of an Outbursting 12.8 Minute Ultracompact X-Ray Binary\*

Paweł Pietrukowicz , Przemek Mróz , Andrzej Udalski, Igor Soszyński , and Jan Skowron 

Warsaw University Observatory, Al. Ujazdowskie 4, 00-478 Warszawa, Poland; [pietruk@astrouw.edu.pl](mailto:pietruk@astrouw.edu.pl)

Received 2019 May 23; revised 2019 July 22; accepted 2019 July 31; published 2019 August 21

## Abstract

We report the discovery of OGLE-UCXB-01, a 12.8 minute variable object located in the central field of Galactic bulge globular cluster Djorg 2. The presence of frequent, short-duration brightenings at such an ultrashort period in long-term OGLE photometry together with the blue color of the object in *Hubble Space Telescope* images and the detection of moderately hard X-rays by *Chandra* observatory point to an ultracompact X-ray binary system. The observed fast period decrease makes the system a particularly interesting target for gravitational-wave detectors such as the planned Laser Interferometer Space Antenna.

*Key words:* binaries (including multiple): close – globular clusters: individual (Djorg 2) – X-rays: binaries

## 1. Variable Stars and the OGLE Survey

Stellar astrophysics owes a lot to observations of variable stars since they provide valuable information on stellar interiors and evolution of single and binary systems. Regular photometric observations of millions of stars help to improve statistics on known variables and to discover rare objects. The OGLE project is a long-term variability survey of the Magellanic System and Milky Way stripe visible from Las Campanas Observatory, Chile. The original science goal of the project in 1992 was a monitoring of the Galactic bulge in searches for microlensing events. That area remains the most frequently observed part of the sky by OGLE with a cadence as short as 20 minutes in the most crowded fields. Since 2010 March the project is in its fourth phase (OGLE-IV; Udalski et al. 2015). OGLE operates the 1.3 m Warsaw telescope equipped with a 32-detector mosaic camera of a total field of view of  $1.4 \text{ deg}^2$  and a pixel size of  $0''.26$ . The previous phase, OGLE-III, was conducted in the years 2001–2009 (Udalski et al. 2008). A significant fraction of OGLE exposures is collected in the Cousins *I* band, while the remaining exposures are taken in the Johnson *V* band. Reductions are performed using the difference image analysis (DIA) technique (Alard & Lupton 1998; Woźniak 2000), developed especially for dense stellar fields.

OGLE has discovered and classified over one million variable stars of various types, including transient, irregular, and periodic objects (e.g., Soszyński et al. 2014, 2015; Mróz et al. 2015). Although the sampling of OGLE observations is not adapted for the detection of millimagnitude variations on timescales of minutes, short-period variable sources with amplitudes of tenths of a magnitude have been found. For example, Pietrukowicz et al. (2017) announced the discovery of blue large-amplitude pulsators (BLAPs), hot pulsating stars with periods in the range 20–40 minutes and optical amplitudes of 0.2–0.4 mag.

## 2. Detection of the Unique Variable

In this Letter, we report the discovery of an unusual periodic variable object with the shortest period ever detected in the OGLE data, that is about 12.79 minutes. A search for short-period objects was carried out for the Galactic bulge data covering OGLE-IV seasons 2010–2013. Around 400 million *I*-band light curves were analyzed in the frequency space from 30 to  $100 \text{ days}^{-1}$  using the FNPEAKS<sup>1</sup> code. It calculates Fourier amplitude spectra of unequally spaced time-series data composed of a large number of points ( $10^4$  or more). The code substantially reduces (by a factor of five) the computation time for a discrete Fourier transform by coadding correctly phased, low-resolution Fourier transforms of pieces of the large data set interpolated to high resolution. OGLE light curves with the resulting highest signal-to-noise ratio were subjected to visual inspection. Among the identified variable stars were BLAPs (Pietrukowicz et al. 2017). Here, particular attention is paid to the detection BLG511.06.25872 (in the OGLE database, detection #25872 in chip 06 of the Galactic bulge field BLG511). Accurate period determination together with the estimation of its uncertainty was performed with the TATRY code (Schwarzenberg-Czerny 1996). It employs periodic orthogonal polynomials to fit the data and the analysis of variance (ANOVA) statistic to evaluate the quality of the fit. Due to the very short period of the variable object, all moments were converted from Heliocentric Julian Date (HJD) to Barycentric Julian Date ( $\text{BJD}_{\text{TDB}}$ ). The true period turned out to be even shorter than the minimum searched period of 14.4 minutes, and the detected signal was an alias (see the power spectrum and phased OGLE light curves in Figure 1). We notice that the reported period is the only one seen in this star. Any longer period would be detected in the OGLE data.

The variable is located in the field of Galactic bulge globular cluster Djorg 2 (ESO 456-SC38) at an angular distance of  $0'.30$  from its center or at  $0.91r_c$ , where the cluster core radius  $r_c = 0'.33$  (from the 2010 version of the catalog by Harris 1996). However, it was not possible to point the true source in ground-based frames due to severe blending. Fortunately, the field of Djorg 2 was imaged with the *Hubble Space Telescope* (*HST*) under program GO 14074. The cluster was observed with the Wide Field Camera of the Advanced

\* Based on observations obtained with the 1.3-m Warsaw telescope at the Las Campanas Observatory of the Carnegie Institution for Science and archival data from NASA/ESA Hubble Space Telescope under program GO 14074 and Chandra X-ray Observatory under program GO 17844.

<sup>1</sup> <http://helas.astro.uni.wroc.pl/deliverables.php?lang=en&active=fnpeaks>

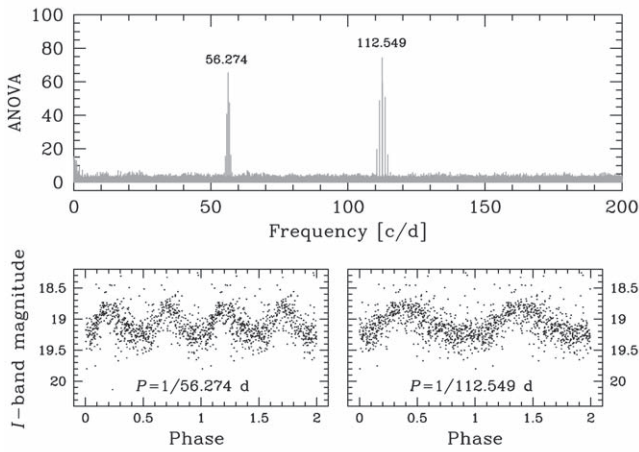


**Figure 1.** ANOVA power spectrum of the discovered variable object (upper panel). The variability was detected at a frequency of 56.274 cycles per day, corresponding to the period of 25.59 minutes, but the true modulation is at 112.549 c/d or the period of 12.79 minutes. Lower panels: phased *I*-band light curve with the two periods. The presented data come from 2017.

Camera for Surveys (ACS/WFC) in the optical filter F606W (corresponding to broad *V*) on 2016 August 19. A week later, on 2016 August 26, it was observed in near-infrared filters with the Wide Field Camera 3 (WFC3/IR), F110W (covering *ZY* bands), and F160W (*H* band). The *HST* data allowed us to indicate the true variable star (see Figure 2) at position  $(x, y) = (2368, 2588)$  in the ACS/WFC drizzled image jcx324010 or at the equatorial coordinates  $(\alpha, \delta)_{2000.0} = (18:01:50.30, -27:49:24.1)$ .

### 3. Investigation of the Nature of the New Object

The object is a periodic variable with an ultrashort period of about 12.79 minutes. Long-term OGLE observations provide some more interesting information (see Figure 3). In the time domain, we can notice short brightenings. They last up to several hours and reach about 1 mag in the *I* band. Due to severe blending, the true amplitude of the brightenings is likely much higher, 2 mag or even more. Another finding is that the period of the variable decreases constantly with a rate of  $-9.16(16) \times 10^{-11} \text{ s s}^{-1}$ . We phased light curves from each OGLE-IV season (2010–2018) separately, cleaned them from outlying points (with  $3\sigma$  clipping) and combined all of them together to one plot (Figure 4). Finally, we fit a third-order Fourier series to the data. The combined *I*-band light curve shows a 0.37 mag bump covering more than half of the period. The bump is slightly more steep on the raising branch and the minimum is almost flat. We note that the observed scatter in the ground-based light curve stems from various reasons: blending, nonnegligible exposure time in comparison to the variability period (100 s versus 767.4 s), and the period decrease. In Table 1, we compile period values of the variable star determined from the OGLE photometry over the years 2004–2018.

Due to significant blending, the true *I*-band amplitude of the periodic modulation is expected to be much higher. The *HST* WFC3/IR data show that the amplitude is indeed extreme, although we cannot determine its exact value. The observations cover over four variability cycles (Figure 5). Five single images with various exposure times ranging from about 24 to 599 s were obtained in each of the two near-infrared filters, F110W

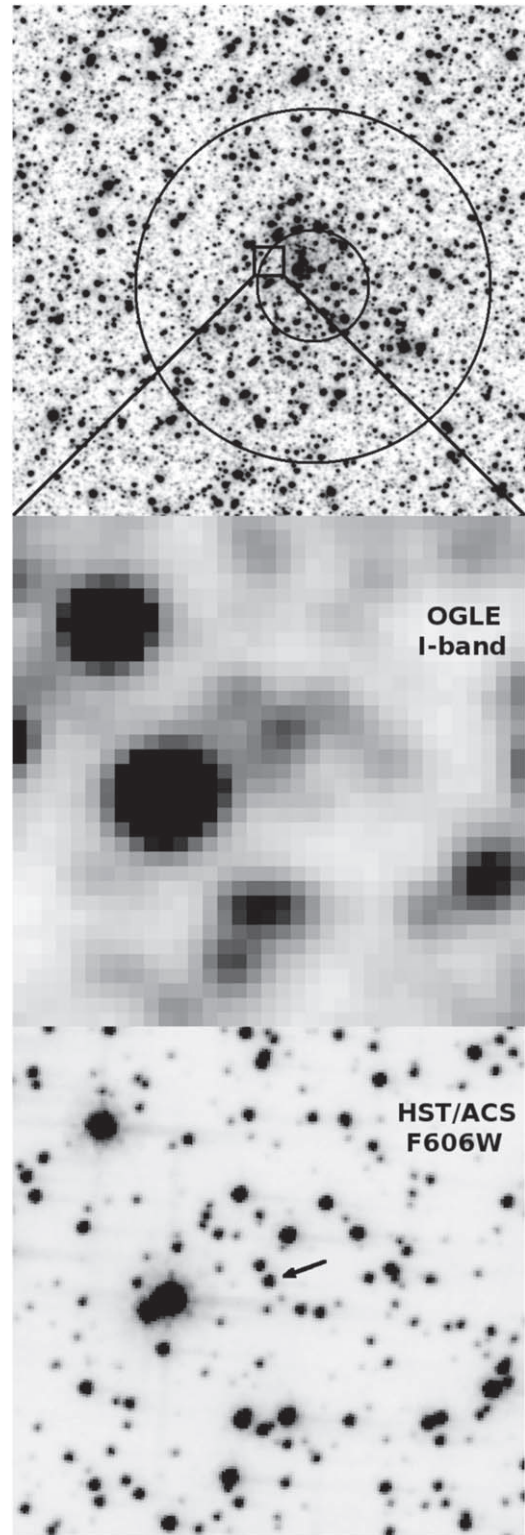


**Figure 2.** Location of the variable object in the field of bulge globular cluster Djorg 2. Upper panel:  $3' \times 3'$  OGLE *I*-band chart centered on the variable with marked core and half-light circle of the cluster. North is up and east to the left. Middle panel:  $9'' \times 9''$  zoom on the variable that could not be resolved in the ground-based image. Lower panel: cropped *HST* ACS/WFC image taken in the F606W filter (broad *V* band) and covering the same small area. The variable star is indicated with the arrow. The closest neighbor, located  $0''.3$  northeast of the variable, served as a comparison star.

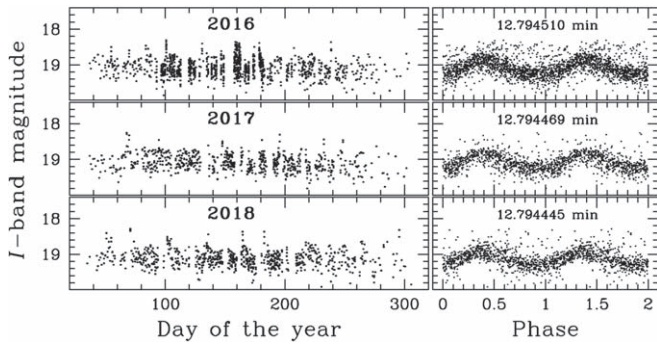


**Figure 3.** OGLE *I*-band light curves of the detected variable from seasons 2016–2018 in the time domain (on the left) and phased with a proper period (on the right). The presence of outbursts at such short period points to an ultracompact system. Due to severe blending the real amplitudes of the outbursts and periodic modulation are expected to be much higher.

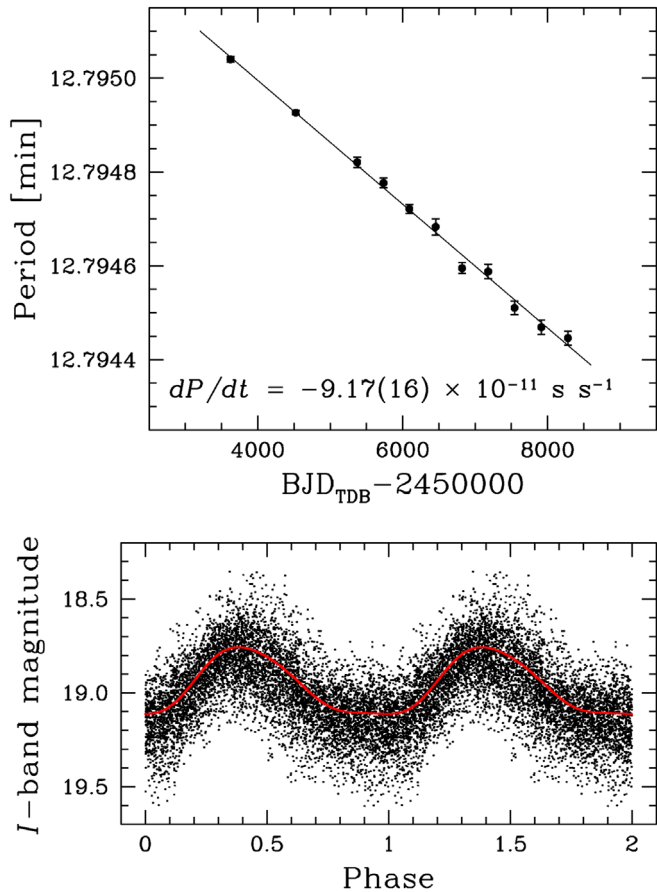


**Figure 4.** Upper panel: constant period decrease observed in the discovered system. Two points from OGLE-III are averaged over the years 2004–2006 and 2007–2009, while nine points from OGLE-IV are averaged over each year from 2010 to 2018, separately. Lower panel: combination of phased *I*-band light curves from OGLE-IV seasons 2010–2018 together with the best fit (red line). Each light curve was cleaned from outbursts and outlying points.

and F160W. We determined magnitudes of the variable star by fitting the point-spread function using the DOLPHOT package (Dolphin 2000). The WFC3 magnitudes roughly reflect variations expected from the long-term OGLE observations. However, one has to remember that the used *HST* filters are centered on longer wavelengths ( $\lambda_{F110W} = 1150$  nm,  $\lambda_{F160W} = 1545$  nm) in comparison to the OGLE *I*-band filter ( $\lambda_I = 800$  nm). The largest difference in brightness reaches

**Table 1**  
Period of the Variable Object in the Years 2004–2018

Years	OGLE Phase	BJD <sub>middle</sub>	<i>P</i> (minutes)	<i>N</i> <sub>obs</sub>
2004–06	III	3624.0977	12.795040(6)	427
2007–09	III	4524.2197	12.794926(4)	583
2010	IV	5372.5320	12.794820(11)	653
2011	IV	5735.7050	12.794776(10)	818
2012	IV	6092.0027	12.794721(10)	918
2013	IV	6455.5293	12.794683(17)	881
2014	IV	6820.4535	12.794594(11)	845
2015	IV	7180.4325	12.794587(15)	804
2016	IV	7544.2946	12.794510(14)	1132
2017	IV	7913.4080	12.794469(15)	692
2018	IV	8281.0703	12.794445(15)	726

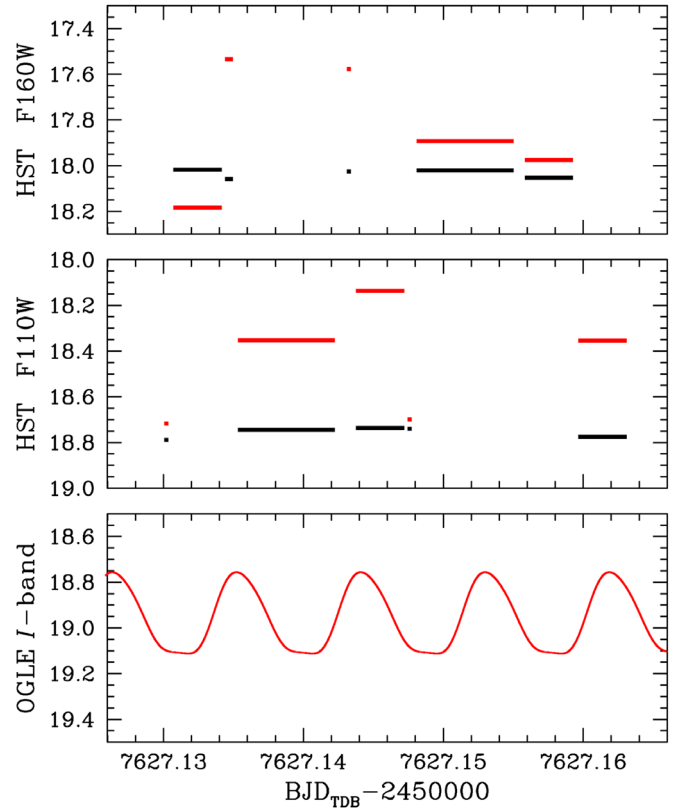


**Figure 5.** Brightness measurements of the discovered object (red lines) and the comparison star (black lines) obtained from the *HST* WFC3/IR observations in F160W filter (upper panel) and F110W filter (middle panel) in comparison with *I*-band variations predicted from the long-term OGLE data (lower panel). Sections correspond to the start–end moments of the executed single *HST* exposures. The measured brightness variations exceed 0.6 mag and are in agreement with the predictions from OGLE. The nearby comparison star seems to be constant.

0.58 mag in F110W and 0.65 mag in F160W, but the true amplitudes are likely slightly higher.

To obtain more information on the nature of the variable object we constructed a color–magnitude diagram based on the *HST* WFC3/IR data (Figure 6). As mean magnitudes of the variable, we adopted values determined from the longest F110W and F160W exposures (599 s), since these cover a major fraction of the period ( $\approx 78\%$ ). In the diagram, the object is located at (F110W–F160W, F110W) = (0.459, 18.352), which is about 0.25 mag blueward of the main-sequence

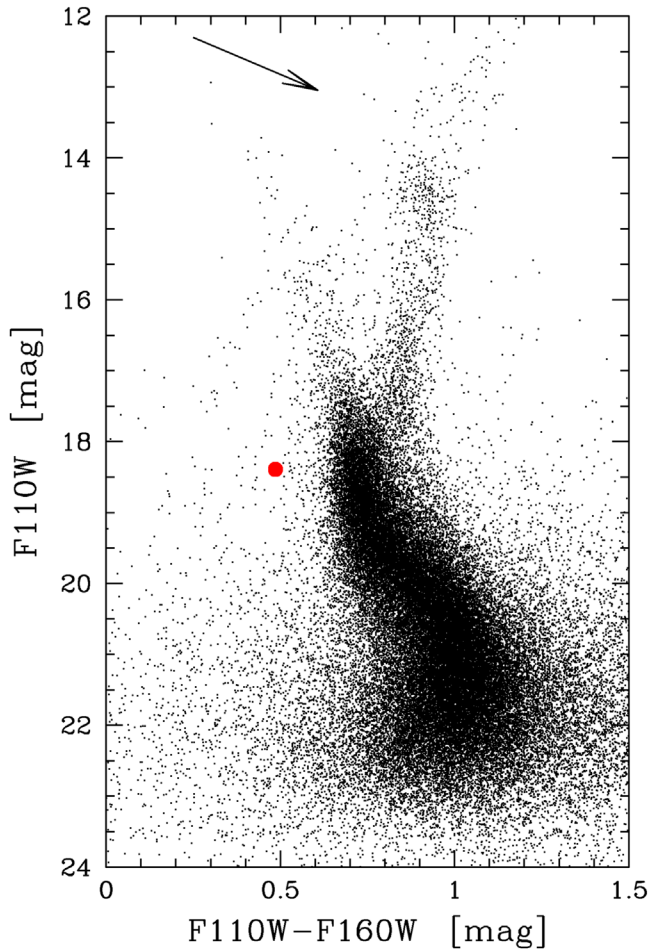


**Figure 6.** Color–magnitude diagram constructed based on *HST* WFC3/IR data for the cluster field with the marked location of the discovered ultracompact system (red dot). Its position  $\approx 0.25$  mag blueward of the main-sequence turnoff shows that this is a hot object. The arrow represents the reddening vector in the direction of the variable object as determined from maps in Nataf et al. (2013) and Nataf (2015).

turnoff point. This position shows that our object is hot. For comparison, the neighboring constant star located  $0''.3$  north-east of the variable can be found well within the main sequence at  $(F110W-F160W, F110W) = (0.724, 18.745)$ .

We notice that the investigated system emits X-rays. The area of globular cluster Djorg 2 was exposed by the *Chandra* satellite observatory for 22.67 ks (about 6.3 hr) on 2017 May 13. There is only one faint ( $0.021 \pm 0.001$  cts  $s^{-1}$ ) point X-ray source detected within the cluster area and located  $0''.64$  from the position of the variable star. We used CIAO 4.11 software (Fruscione et al. 2006) and CALDB version 4.8.3 to extract the X-ray spectrum of the source, which is shown in the upper panel of Figure 7. The spectrum can be well described by an absorbed power law with the photon index  $\Gamma = 1.22 \pm 0.23$ . The estimated equivalent hydrogen column density ( $N_H = (0.53 \pm 0.20) \times 10^{22}$   $cm^{-2}$ ) is consistent with the interstellar extinction toward the cluster. The X-ray modeling was performed using the SHERPA package (Freeman et al. 2001). The total unabsorbed flux in the range 0.5–10 keV is  $4.8^{+0.5}_{-0.6} \times 10^{-13}$   $erg s^{-1} cm^{-2}$ , which corresponds to the luminosity of  $4.4 \pm 0.5 \times 10^{33}$   $erg s^{-1}$ , assuming the source is associated with the cluster at the distance of 8.75 kpc (Ortolani et al. 2019). In the lower panel of Figure 7, we compare the

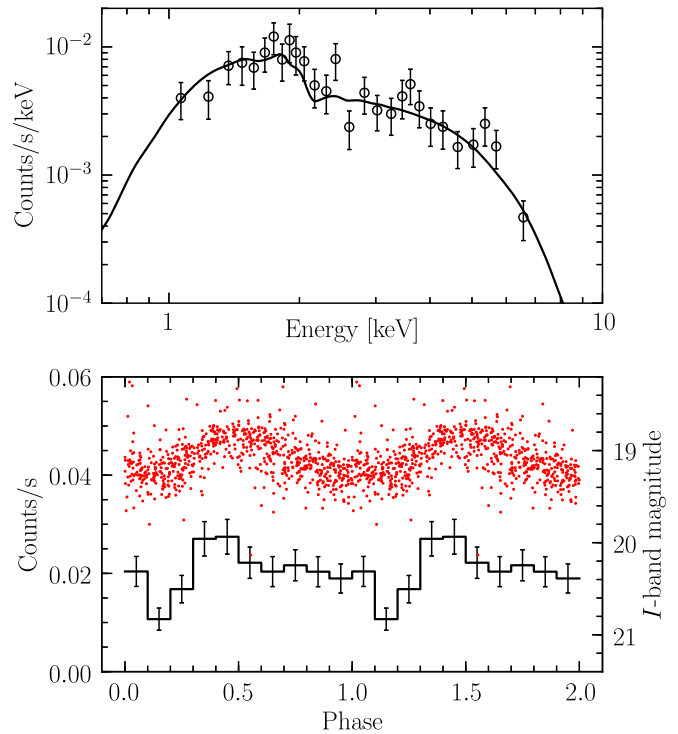


**Figure 7.** Spectral energy distribution (upper panel) and phase distribution (lower panel) of the X-rays detected with *Chandra* observatory at the location of the discovered system. The X-ray spectrum can be described by an absorbed power law with the photon index  $\Gamma = 1.22 \pm 0.23$ . The X-ray signal correlates with the optical variability observed by OGLE. The energy distribution is very similar to the distributions observed in known ultracompact X-ray binaries. Therefore, we name the new system OGLE-UCXB-01.

phased X-ray light curve with the optical light curve from 2017. We applied a barycentric correction to the data. Correlation between the X-ray and optical signal is strong with a coefficient of 0.72, as obtained after binning both phased light curves into 10 bins.

#### 4. Conclusions

All facts reported above indicate that the discovered OGLE variable object is a UCXB. UCXBs are a subgroup of low-mass X-ray binaries (LMXBs) in which the primary component is either a black hole or a neutron star. Lack of other periodicities in the long-term OGLE photometry means that the 12.79 minute signal represents the orbital period of the binary. Spin period of the primary is likely too short to be detected in the OGLE data. X-ray emission is evidence for accretion processes in the system. The presence of brightenings lasting several hours and the light curve shape in the optical regime point to a small accretion disk around the primary. Our object cannot be a close cataclysmic system of AM CVn type formed of a white dwarf accretor and a degenerate helium-rich donor. In such systems, outbursts do not occur at orbital periods shorter than about 20 minutes (Solheim 2010; Ramsay et al. 2018) and the X-ray spectrum is softer, with a peak around or below 1 keV (e.g., Strohmayer 2004; Ramsay et al. 2006). We name the newly discovered object OGLE-UCXB-01.

About a third of known UCXBs were found in globular clusters (Nelemans & Jonker 2010). For instance, the prototype of the whole group, 4U 1820-30 or Sgr X-4, resides in Galactic bulge globular cluster NGC 6624 (Stella et al. 1987). OGLE-UCXB-01 is observed within the core radius of cluster Djorg 2.





It may belong to this cluster. Assuming the distance to Djorg 2 is 8.75 kpc (Ortolani et al. 2019) and approximate extinction in this direction  $A_V \approx 2.4$  mag (based on the interstellar calculator provided in Nataf et al. 2013), we find that the star with the observed brightness  $F606W \approx 21.2$  mag (broad  $V$  band) would have an absolute brightness  $M_V \approx +4.1$  mag, which is a typical value for UCXBs (Nelemans & Jonker 2010).

We could consider the possibility that the new object is a binary system containing a slowly rotating spinning-up accreting neutron star. The observed optical modulation would be the spin period of the neutron star with the measured spin-up rate. In this interpretation, however, it is difficult to explain the absence of a longer modulation representing the orbital period of the system. Nevertheless, the newly detected object requires an optical spectrum that may reveal chemical composition of the accreted matter. Long-term X-ray monitoring would allow searching for X-ray bursts and their possible correlation with optical outbursts. Radial velocity and proper motion measurements should provide the answer to the question whether the object belongs to globular cluster Djorg 2. OGLE-UCXB-01 as an ultracompact low-mass binary with a fast period decrease is expected to be a strong gravitational-wave source in the low-frequency regime. Once the cluster membership is confirmed or the distance to the system is well determined, the object may serve as a verification target for planned space mission LISA.

We thank Prof. Tomek Bulik for discussions on the nature of the discovered system, and Dr. Szymon Kozłowski for help in the reduction of the HST data. We thank OGLE observers for their contribution to the collection of the photometric data over the years. The OGLE project has received funding from the National Science Centre, Poland (grant number MAESTRO 2014/14/A/ST9/00121 to A.U.). P.M. acknowledges support from the Foundation for Polish Science (Program START). This Letter makes use of observations from the NASA/ESA *Hubble Space Telescope*, obtained at the Space Telescope

Science Institute, which is operated by the Association of Universities for Research in Astronomy, Inc., under NASA contract NAS 5-26555. The *HST* observations are associated with program GO 14074. Some scientific results reported in this Letter are based on data obtained from the *Chandra* Data Archive, under program GO 17844.

### ORCID iDs

Pawel Pietrukowicz  <https://orcid.org/0000-0002-2339-5899>  
 Przemek Mróz  <https://orcid.org/0000-0001-7016-1692>  
 Igor Soszyński  <https://orcid.org/0000-0002-7777-0842>  
 Jan Skowron  <https://orcid.org/0000-0002-2335-1730>

### References

- Alard, C., & Lupton, R. H. 1998, *ApJ*, 503, 325  
 Dolphin, A. E. 2000, *PASP*, 112, 1383  
 Freeman, P., Doe, S., & Siemiginowska, A. 2001, *Proc. SPIE*, 4477, 76  
 Fruscione, A., McDowell, J. C., Allen, G. E., et al. 2006, *Proc. SPIE*, 6270, 62701V  
 Harris, W. E. 1996, *AJ*, 112, 1487  
 Mróz, P., Udalski, A., Poleski, R., et al. 2015, *AcA*, 65, 313  
 Nataf, D. M. 2015, *MNRAS*, 449, 1171  
 Nataf, D. M., Gould, A., Fouqué, P., et al. 2013, *ApJ*, 769, 88  
 Nelemans, G., & Jonker, P. G. 2010, *NewAR*, 54, 87  
 Ortolani, S., Held, E. V., Nardiello, D., et al. 2019, *A&A*, 627, A145  
 Pietrukowicz, P., Dziembowski, W. A., Latour, M., et al. 2017, *NatAs*, 1, 166  
 Ramsay, G., Green, M. J., Marsh, T. R., et al. 2018, *A&A*, 620, A141  
 Ramsay, G., Groot, P. J., Marsh, T., et al. 2006, *A&A*, 457, 623  
 Schwarzenberg-Czerny, A. 1996, *ApJL*, 460, L107  
 Solheim, J.-E. 2010, *PASP*, 122, 1133  
 Soszyński, I., Udalski, A., Szymański, M. K., et al. 2014, *AcA*, 64, 177  
 Soszyński, I., Udalski, A., Szymański, M. K., et al. 2015, *AcA*, 65, 297  
 Stella, L., White, N. E., & Priedhorsky, W. 1987, *ApJL*, 315, L49  
 Strohmayer, T. E. 2004, *ApJ*, 614, 358  
 Udalski, A., Szymański, M. K., Soszyński, I., & Poleski, R. 2008, *AcA*, 58, 69  
 Udalski, A., Szymański, M. K., & Szymański, G. 2015, *AcA*, 65, 1  
 Woźniak, P. R. 2000, *AcA*, 50, 421